

Metabolic effect of alkaline additives and guanosine/gluconate in storage solutions for red blood cells

Angelo D'Alessandro,¹ Julie A. Reisz,¹ Rachel Culp-Hill,¹ Herbert Korsten,²
Robin van Bruggen,^{3,4} and Dirk de Korte^{2,3,4}

BACKGROUND: Over a century of advancements in the field of additive solutions for red blood cell (RBC) storage has made transfusion therapy a safe and effective practice for millions of recipients worldwide. Still, storage in the blood bank results in the progressive accumulation of metabolic alterations, a phenomenon that is mitigated by storage in novel storage additives, such as alkaline additive solutions. While novel alkaline additive formulations have been proposed, no metabolomics characterization has been performed to date.

STUDY DESIGN AND METHODS: We performed UHPLC-MS metabolomics analyses of red blood cells stored in SAGM (standard additive in Europe), (PAGGSM), or alkaline additives SOLX, E-SOL 5 and PAG3M for either 1, 21, 35 (end of shelf-life in the Netherlands), or 56 days.

RESULTS: Alkaline additives (especially PAG3M) better preserved 2,3-diphosphoglycerate and adenosine triphosphate (ATP). Deaminated purines such as hypoxanthine were predictive of hemolysis and morphological alterations. Guanosine supplementation in PAGGSM and PAG3M fueled ATP generation by feeding into the nonoxidative pentose phosphate pathway via phosphoribolysis. Decreased urate to hypoxanthine ratios were observed in alkaline additives, suggestive of decreased generation of urate and hydrogen peroxide. Despite the many benefits observed in purine and redox metabolism, alkaline additives did not prevent accumulation of free fatty acids and oxidized byproducts, opening a window for future alkaline formulations including (lipophilic) antioxidants.

CONCLUSION: Alkalinization via different strategies (replacement of chloride anions with either high bicarbonate, high citrate/phosphate, or membrane impermeant gluconate) results in different metabolic outcomes, which are superior to current canonical additives in all cases.

One hundred years of advancements in the field of transfusion medicine and, in particular, storage additives for red blood cells (RBCs)¹⁻³ have made transfusion therapy a safe and effective mainstay of current medical practice for over 11 million Americans every year.⁴ In 1981 the first modern-era additive containing saline, adenine, glucose, and mannitol (SAGM) was formulated. This allowed storage of RBCs for up to 6 weeks owing to the role of mannitol in balancing osmolarity and decreasing hemolysis.⁵ A similar additive solution (AS-1) to SAGM was subsequently formulated in the United States.⁶ AS-3 and AS-5⁶⁻⁸ were designed in the subsequent decades, with AS-3 containing phosphate buffers and citrate (instead of mannitol) to fuel synthesis of high-energy phosphate compounds and make this additive more viable to pediatric patients, respectively. Over the years, SAGM modifications have been formulated, including guanosine as a source of ribose phosphate secondary to phosphoribolysis (PAGGSM),

ABBREVIATIONS: DPG = diphosphoglycerate; GSSG = glutathione disulfide; PLS-DA = partial least square-discriminant analysis; PPP = pentose phosphate pathway; PS = phosphatidylserine.

From the ¹Department of Biochemistry and Molecular Genetics, University of Colorado Denver—Anschutz Medical Campus, Aurora, Colorado; and the ²Department of Product and Process Development, Sanquin Blood Bank; the ³Department of Blood Cell Research, Sanquin Research; and ⁴Landsteiner Laboratory, Academic Medical Centre, Amsterdam, the Netherlands.

Address reprint requests to: Angelo D'Alessandro, Department of Biochemistry and Molecular Genetics, University of Colorado Denver, Anschutz Medical Campus, Aurora, CO 80045; e-mail: angelo.dalessandro@ucdenver.edu.

Received for publication January 18, 2018; revision received March 1, 2018; and accepted March 1, 2018.

doi:10.1111/trf.14620

© 2018 AABB

TRANSFUSION 2018;58:1992-2002

which thus sustains late adenosine triphosphate (ATP)-generating glycolysis reactions without the need for a net expenditure of ATP.⁹ More recently, novel additives such as AS-7 (commercial name SOLX)¹⁰ or erythrosol-5 (E-SOL 5)¹¹ were designed building on the concept of chloride shift¹²⁻¹⁴—which favors intracellular pH alkalization by promoting chloride efflux in low-chloride/chloride-free/high-bicarbonate additives—with beneficial effects to energy and redox metabolism (reviewed here).¹⁵ Similar effects could be obtained by replacing the saline component with salt-containing membrane-impermeant anions such as sodium gluconate, which generates a reversible intracellular alkalosis.¹⁶⁻¹⁸

With over 112.5 million units donated globally every year and an average end-of-storage loss of potency of at least approximately 17%¹⁹ in current additives (calculated from posttransfusion recovery studies),²⁰ novel storage additives still offer an actionable window of opportunity to significantly impact the field of transfusion medicine by improving RBC storage quality.²¹ Alterations of purine metabolism resulting from ATP consumption and breakdown into purines like hypoxanthine are markers of the metabolic age of RBCs.²² Decreases in the levels of non-deaminated purines cannot be corrected by additional adenine loading of storage additives.²³ Activation of purine deaminases such as erythrocyte-specific adenosine monophosphate (AMP) deaminase 3 in turn results in potentially toxic by-products such as hypoxanthine. Hypoxanthine has been recently identified as a negative predictor of posttransfusion recovery in stored mouse and human RBCs²⁴ and a substrate for circulating xanthine oxidase for the generation of urate and hydrogen peroxide.²⁵ In this view, end-of-storage rejuvenation of RBCs has been proposed, which exploits inosine and pyruvate to replenish late glycolysis via phosphoribolysis-derived pentose phosphate sugars and to promote oxidation of NADH back to NAD⁺ via lactate dehydrogenase, respectively. However, excess inosine transformation to hypoxanthine results in the necessity to wash rejuvenated units prior to transfusion.²⁶

In addition, the use of alternative sugars (or sugar alcohols) instead of glucose, such as mannose, fructose, or sorbitol (as a replacement for mannitol)^{27,28} has been proposed as a viable strategy to bypass early glycolytic blockade promoted by feedback inhibition of phosphofructokinase by intracellular acidification, a mechanism evolutionarily exploited by animals such as naked mole-rats to resist extreme anoxia.²⁹ Finally, antioxidants such as vitamin C, N-acetylcysteine, and vitamin E have been proposed as additives for RBC storage in that they attenuate the oxidative storage lesion, especially to the lipid component,³⁰⁻³⁴ which is relevant in the light of the correlation between lipid oxidation and posttransfusion recovery.³⁵

The current availability of new “omics” technologies is providing increased understanding of the RBC proteome and metabolome.^{36,37} For example, although RBCs lack mitochondria, they have now been shown to metabolize carboxylic acids from citrated anticoagulants or storage additives^{38,39} in an oxygen-dependent fashion.⁴⁰ Omics technologies have helped investigators in the field of transfusion medicine to characterize the multifaceted nature of the storage lesion⁴¹ and, by qualitatively and quantitatively characterizing its evolution in different storage additives,⁴²⁻⁴⁵ pave the way for future developments in the field. Recently, we performed a comparative analysis of hemolysis, ion homeostasis, and osmotic fragility of RBCs stored in five different additives.⁴⁶ Here, we expand on those observations by providing metabolomics evidence of the beneficial effects of alkaline additives when compared to AS-3 and correlating metabolomics data to previously measured functional parameters.

MATERIALS AND METHODS

Commercial reagents were purchased from Sigma-Aldrich unless otherwise noted.

Blood collection, processing, and storage

Blood collection, processing, and storage were described in detail elsewhere.⁴⁶ Briefly, 500 mL blood in citrate-phosphate-dextrose (CPD) anticoagulant was collected from healthy, volunteer, donors ($n = 15$) in accordance with the Declaration of Helsinki. For each series, three series of replicates consisting of 5 ABO-compatible pooled blood units were split, plasma and buffy coat depleted. Subsequently, 110 mL was added of the various additive solutions SAGM, E-SOL5, PAGGSM (Fresenius Kabi, Emmer-Compascuum), SOLX (AS-7) or PAGGGM (both prepared in house), followed by leukoreduction ($<1 \times 10^6$ remaining white blood cells [WBCs]). Formulations of the additive solutions are extensively described by Lagerberg and colleagues.⁴⁶ Units were aseptically sampled at Storage Days 1, 21, 35 (end of shelf life for RBCs in the Netherlands), and 56 days. The rationale behind this sampling timeline was informed by the observation that “the decline in 2,3-DPG was inhibited during storage in E-Sol 5 and AS-7, while in PAG3M, 2,3-DPG level increased above the initial level till day 35 and remained detectable till day 56,” as reported by Lagerberg and colleagues.⁴⁶ Here, we wanted to test whether these observations for 2,3-diphosphoglycerate (DPG) could be also expanded to other metabolic pathways. RBCs and supernatants were separated by centrifugation at $2000 \times g$ for 10 minutes at 4°C at each time point, and the RBC pellets were shipped frozen to the metabolomics facility to be processed for metabolomics analyses as described below.

Osmotic fragility, morphology, and gas measurements were performed as previously reported.⁴⁶

Metabolite extraction

A volume of 50 μ L of RBCs was extracted in 450 μ L of lysis buffer (methanol:acetonitrile:water 5:3:2), before ice cold extraction by vortexing for 30 minutes at 4°C.^{15,38} Insoluble proteins were pelleted by centrifugation (10 minutes at 4°C and 10,000 \times g) and supernatants were collected and stored at -80°C until analysis.

UHPLC-MS metabolomics

Analyses were performed using a liquid chromatography system (Vanquish UHPLC, Thermo Fisher) coupled online to a mass spectrometer (Q Exactive, Thermo Fisher). Samples were resolved over a core-shell column (2.1 \times 150 mm, 1.7 μ m; Kinetex C18, Phenomenex) at 25°C using a 3-minute isocratic condition of 5% acetonitrile, 95% water, and 0.1% formic acid flowing at 250 μ L/min,⁴⁷ or using a 9-minute gradient at 400 μ L/min from 5% to 95% B (A: water/0.1% formic acid; B: acetonitrile/0.1% formic acid).³⁸ Mass spectrometry analysis and data elaboration were performed as described.³⁸ Metabolite assignments were performed using computer software (MAVEN, Princeton University), as described.⁴⁸

Statistical analyses

Graphs and statistical analyses, including partial least square-discriminant analysis (PLS-DA) and two-factor (time series + one-factor) statistical analysis were performed with computer software (GraphPad Prism 5.0, GraphPad Software, Inc.) and Metaboanalyst 3.0.⁴⁹ Line plots were performed through interpolation of available data points for all tested storage days (third-degree polynomials) via GraphPad Prism. Metabolic linkage analyses have been recently described.⁵⁰ Briefly, correlative analyses (Pearson or Spearman correlations— r —upon testing for normality distribution of data with Kolmogorov-Smirnov) and calculation of $\Delta|r|>30\%$ deviations were performed with GraphPad Prism 5.0 and Excel 2017 (Microsoft), while results were plotted with computer software (GENE-E, Broad Institute). Briefly, the underlying assumption of the metabolic linkage analysis⁵⁰ is that even though correlation does not necessarily imply causation, the levels of metabolites from linked pathways are highly correlated owing to biochemical constraints of the enzymatic reactions necessary to consume one metabolite to generate another.

RESULTS

Gas and ion homeostasis, osmotic fragility, phosphatidylserine exposure, and morphology

Hematocrit, mean cell volume (MCV), pH, % hemolysis, osmotic fragility, phosphatidylserine (PS) exposure and

morphologic alterations (reported as percentage of echinocytes) were measured for RBCs stored in different additives (in part previously reported⁴⁶ and here re-elaborated in Figs. S1 and S2, available as supporting information in the online version of this paper). Though limited by the lack of functional *in vivo* measurements of RBC storage quality and transfusion efficacy (e.g., posttransfusion recoveries), the parameters we measured here represent important surrogate indexes of “functional” relevance (e.g., percentage of spontaneous and osmotic hemolysis). Mean cell volume was highest in SAGM RBCs throughout storage (Fig. S2). SAGM RBCs had the highest end-of-storage osmotic fragility, with trends toward increase during storage duration (consistent with previous observations),⁵¹ while other additives showed trends toward decrease (Fig. S1). Alkalinization in the various additives was achieved either by high bicarbonate load (SOLX), low chloride (PAGGSM), or no chloride (PA3GM, SOLX and E-SOL 5; Fig. S2). Lower end-of-storage pH was observed in PAG3M and PAGGSM in comparison to SOLX and E-SOL 5, though trends were mostly comparable across all additives. E-SOL 5 and PAG3M showed the lowest end-of-storage hemolysis and highest—though within a very narrow window range—PS exposure (the latter parameter normalized across additives by incubation at 37°C), despite all additives showing a similar percentage of echinocytes upon morphologic analysis throughout storage (Fig. S1).

Metabolomics overview

Metabolomics analyses were performed at Days 1, 21, 35 (end of standard storage in the Netherlands), and 56. Results are extensively reported in Table S1, available as supporting information in the online version of this paper. Hierarchical clustering of metabolic trends in all additives was performed (Fig. S3, available as supporting information in the online version of this paper) and a detail of the top significant features (repeated measures ANOVA; $p < 0.01$ false discovery rate corrected) is reported in Fig. 1. On the basis of these metabolic phenotypes, we clustered samples via PLS-DA (Fig. 2A; two-dimensional plots for PC1 vs. PC2, PC1 vs. PC3, and PC2 vs. PC3 are reported in Fig. S4 [available as supporting information in the online version of this paper]), showing that PAG3M was the only additive not showing the typical U-shaped progression over PC1 and PC2 previously described by us and others.^{22,43} Notably, glycolytic measurements through classic spectrophotometric approaches and UHPLC-MS (Fig. 2B and C, respectively) concordantly showed higher glucose consumption and generation of ATP, DPG, and lactate in PAG3M, which contained half the initial dose of glucose as SOLX and E-SOL 5. In particular, despite the lower intracellular pH, PAG3M better preserved DPG levels throughout storage, followed by SOLX and E-SOL 5 (Fig. 2B). No significant alterations in reduced to oxidized glutathione ratios (glutathione/

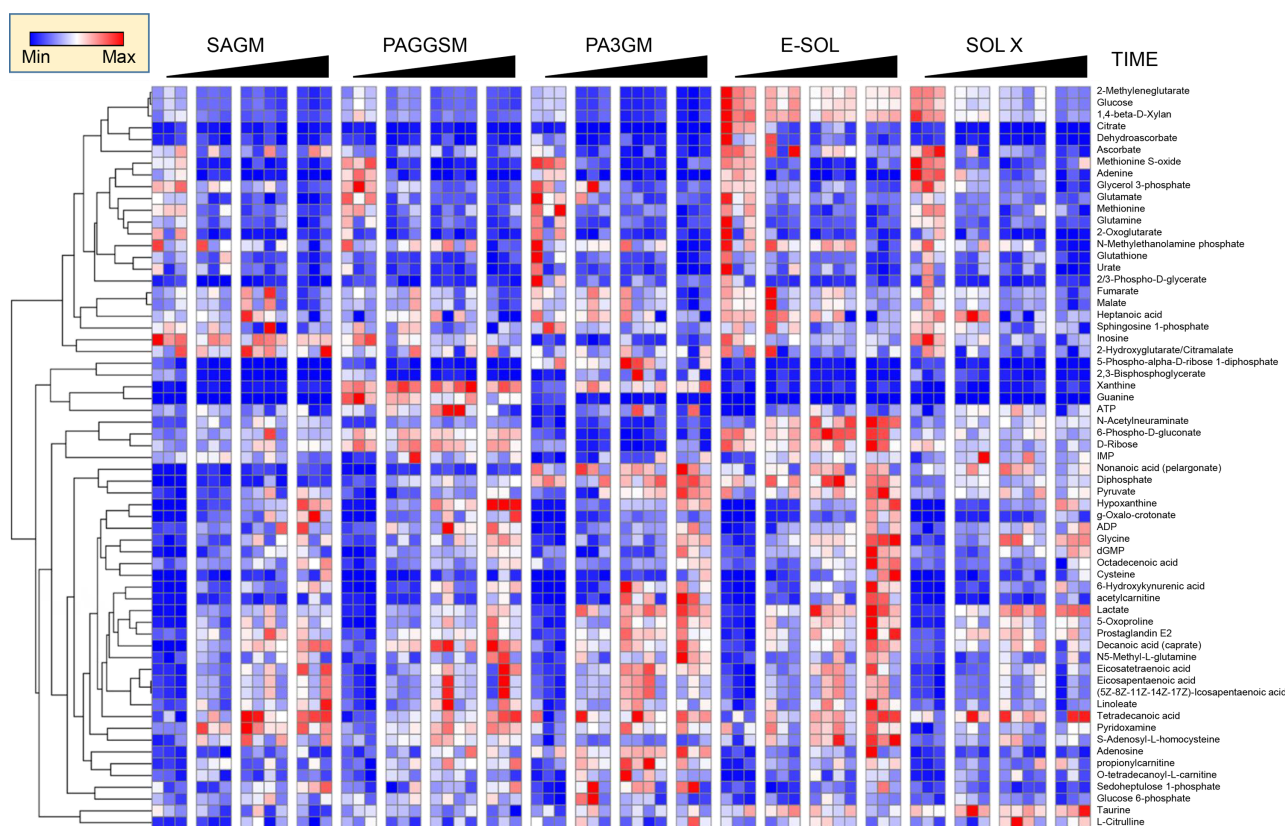


Fig. 1. Hierarchical clustering analyses of time course measurements of RBC metabolites at Storage Days 1, 21, 35, and 56 in five different storage additives. Significant metabolites by ANOVA (false discovery rate corrected) are shown in the heatmap (rows), upon Z-score normalization across all samples and color-coding (blue to red = low to high—legend in the top left corner). A vectorial version of this graph is provided as Fig. S3. [Color figure can be viewed at wileyonlinelibrary.com]

glutathione disulfide [GSSG]) were observed across additives, though PAG3M showed the highest sedoheptulose phosphate/6-phosphogluconate ratio and E-SOL 5 the lowest (Fig. 2C). In the absence of flux data, this observation is suggestive of increased fluxes through the pentose phosphate pathway (PPP) in PAG3M-stored RBCs, suggestive of higher NADPH-generating (i.e., oxidized thiol-reducing) capacity. E-SOL 5 and SOLX had the highest levels of intracellular malate (declining in all additives over storage, likely owing to release in the supernatants), despite higher levels of citrate in the former additive (Fig. 2D).

Metabolic linkage analysis (Fig. 3; extensively described in previous reports)⁵⁰ allows the determination of metabolic reprogramming of RBCs stored in different additives. The underlying rationale for this approach is that biochemical constraints of enzymatic reactions result in strong and significant positive/negative correlations across metabolites in the same pathways, unless the activity of one enzyme in the cascade is up/down regulated by modulatory events (e.g., inactivating oxidation of active site cysteine of glyceraldehyde 3-phosphate dehydrogenase is observed during RBC storage).⁵³ Metabolite levels in SAGM RBCs were correlated to each other, prior to repeating a similar correlation

analysis across all additives while maintaining the order of metabolites of original elaborations in SAGM (Fig. 3A) or performing a hierarchical clustering of correlations in an additive-by-additive fashion (Fig. 3B). This analysis provides at a glance an overview of metabolic rewiring across additives, indicating a strong effect on redox homeostasis, carboxylic acid, fatty acid, and purine metabolism in alkaline additives when compared to SAGM (Fig. 3; Supplementary Table 2). Of note, changes in glutamine metabolism and glutathione homeostasis were observed across additives with respect to total glutathione levels (both reduced and oxidized being lowest in PAGGSM; Fig. S5 [available as supporting information in the online version of this paper]). SAGM showed the highest levels of GSSG for the first 21 days of storage. Cysteine accumulated significantly in E-SOL 5 RBCs over storage duration in comparison to other additives, mainly at outdate of the unit at Storage Day 56 (Fig. S6, available as supporting information in the online version of this paper).

Purine and fatty acid metabolism

Supplementation of guanosine in PAGGSM and PAG3M resulted in significantly higher levels of guanine and

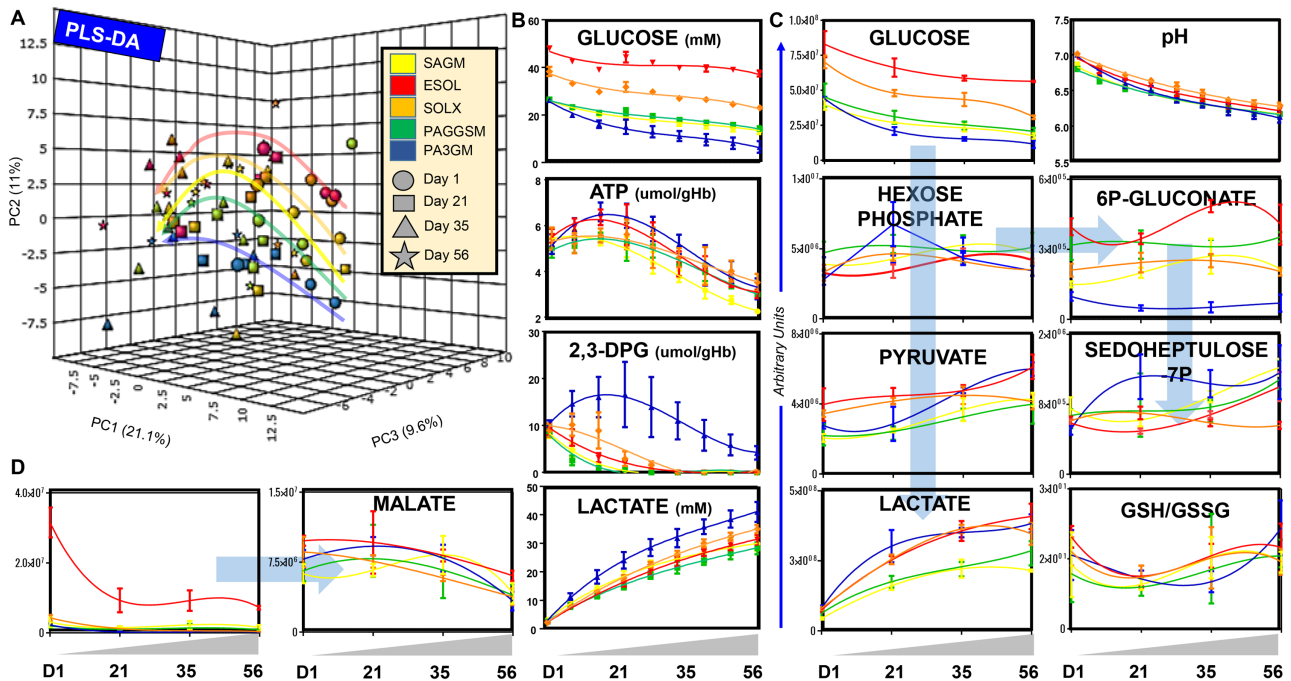


Fig. 2. PLS-DA of metabolomics data from RBCs stored in five additive solutions, following the color code on the right-hand side of panel A. In B, C, and D, line plots indicate median \pm range (continuous \pm error bars) for metabolites involved in glycolysis as measured by classic spectrophotometric approaches (B) or UHPLC-MS (C), and carboxylic acids citrate and malate (D). Color codes are consistent with the legend in A. [Color figure can be viewed at wileyonlinelibrary.com]

adenosine and comparably lower levels of inosine (especially PAG3M) in comparison to all the other additives tested here (Fig. 4). This is suggestive of guanosine from PAGGSM and PAG3M being mostly metabolized via phosphoribolysis rather than hypoxanthine guanosine phosphoribosyl transferase (HGPRT). Deaminated purines (and the ratio of deaminated/nondeaminated purines—e.g., adenosine/inosine; AMP/inosine monophosphate; adenine/hypoxanthine) were the lowest in PAG3M (Fig. 4). On the other hand, urate to xanthine (or hypoxanthine) ratios were the highest in E-SOL 5 and SAGM, followed by SOLX (Fig. 4). Inferring from steady-state data, these results are suggestive of increased purine deamination and catabolism to urate (a reaction that also generates the pro-oxidant hydrogen peroxide) in SAGM and E-SOL 5, in part mitigated by SOLX.

On the other hand, SOLX showed the lowest accumulation of free fatty acids and arachidonic acid peroxidation products, followed by SAGM, PAGGSM, E-SOL 5 and PAG3M (Fig. S3).

Correlation of metabolomics data to functional outcomes

Metabolomics data were correlated to functional outcomes (including energy state as determined by ATP levels, hemolysis, osmotic fragility, PS exposure and

morphological alterations) in additive-dependent (Table S1, Figs. 5 and 6B) and an additive independent fashion (Fig. S7 [available as supporting information in the online version of this paper], Fig. 6A). An overview of top metabolites showing significant positive (red) or negative (blue) correlations to ATP across all additives is provided in Fig. 5A. Of note, most trends observed showed a progression towards increasingly higher (e.g., lactate and ATP; Fig. 5B) or lower (e.g. ATP and sphingosine 1-phosphate) correlations across all additives (Fig. 5A). Correlations between ATP and DPG were poor for all additives except for PAG3M (Fig. 5C), suggesting a rewiring of the Rapoport-Luebering shunt specific to this additive. Of note, purine metabolites (especially ATP, adenosine, and the deamination products inosine and hypoxanthine) were the best correlates with functional outcomes (Fig. 6B), with hypoxanthine being the best predictor of hemolysis and morphological alterations (percentage of echinocytes) in all additives. Of note, inosine was a good predictor of osmotic fragility in all additives except for SAGM (Fig. 6B).

DISCUSSION

In the past few years, metabolomics analyses of stored RBCs have generated a wealth of observational data whose clinical relevance is still matter of debate.⁵⁴ Based on the

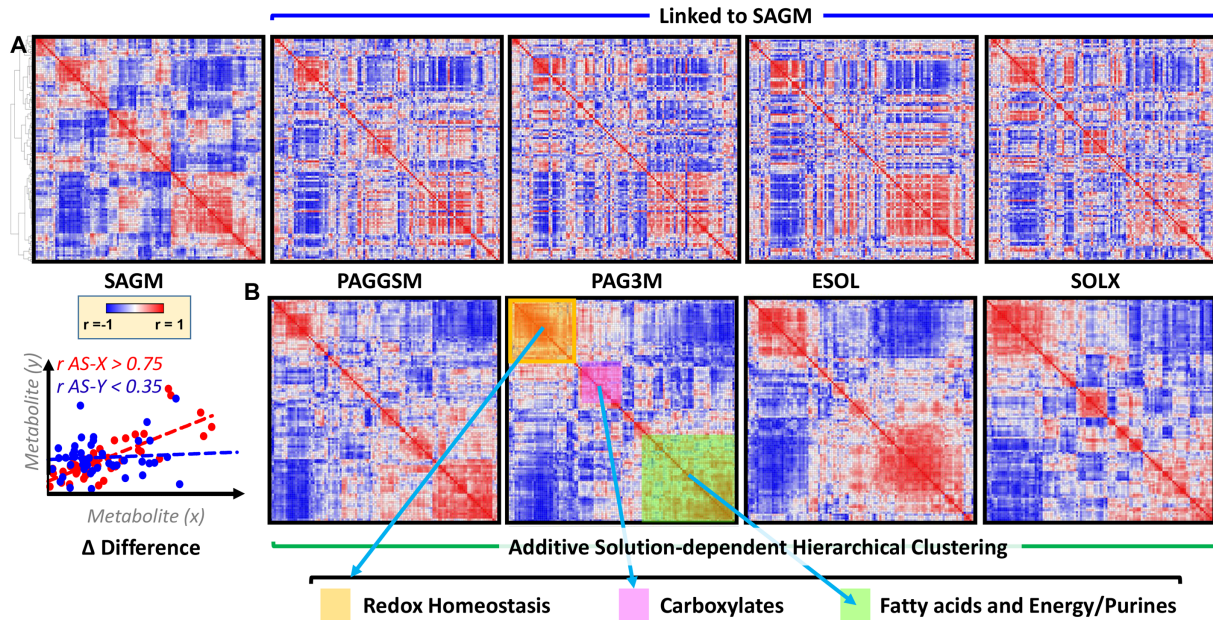


Fig. 3. Metabolic linkage analysis of RBCs stored in five different additive solutions. (A) Metabolites were correlated to each other and results plotted as correlation maps (from blue to red = r from -1 to $+1$; Spearman's correlation). Metabolites were thus hierarchically clustered on the basis of Spearman correlations of all values at any given time point as measured in SAGM. The order of metabolites was thus maintained across all additives, though Spearman correlations were calculated separately for each additive in order to visually show disruption of metabolic linkage⁵⁰ (correlation across metabolites) across the different storage conditions. This analysis allows identification of the disruption of correlations and generation of new ones in response to storage in different additives, an indirect measure of metabolic rewiring. A hypothetical example of two metabolites (x and y) correlating differently between each other under a condition AS-X (in red) and AS-Y (in blue) is provided in the bottom left corner of the figure. (B) Hierarchical clustering of Spearman correlations across all metabolites was independently performed for each additive solution to reveal the formation of new clusters of highly correlated metabolites in alkaline additives involving metabolites from redox homeostasis, carboxylic acids, fatty acid, and purine metabolism. [Color figure can be viewed at wileyonlinelibrary.com]

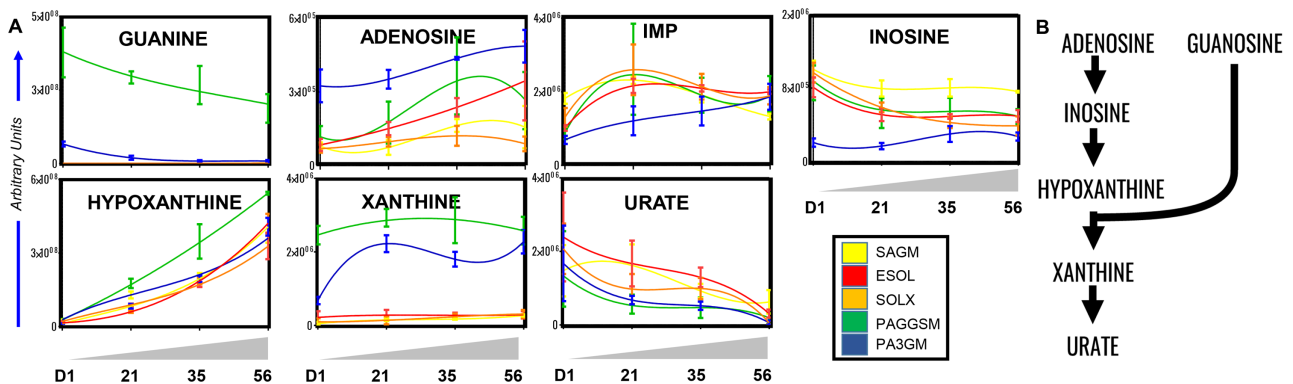


Fig. 4. Purine metabolism. (A) Line plots indicate median \pm range (continuous \pm error bars) for metabolites involved in purine metabolism as measured by UHPLC-MS. Color codes are indicated in the bottom right corner of panel A. (B) Overview of the pathway involving the metabolites graphed in A. [Color figure can be viewed at wileyonlinelibrary.com]

consideration that, in order to transport and deliver oxygen, transfused RBCs must remain intact and circulate in the bloodstream of the recipient, correlative studies have been published in mice and humans suggesting a role for lipid

and purine oxidation (e.g., 5-hydroxyeisosatetraenoic acid and other hydroxyeisosatetraenoic acids, ATP, and hypoxanthine) in mediating RBC hemolysis and posttransfusion recovery.^{24,35,55,56} These observations are relevant in that

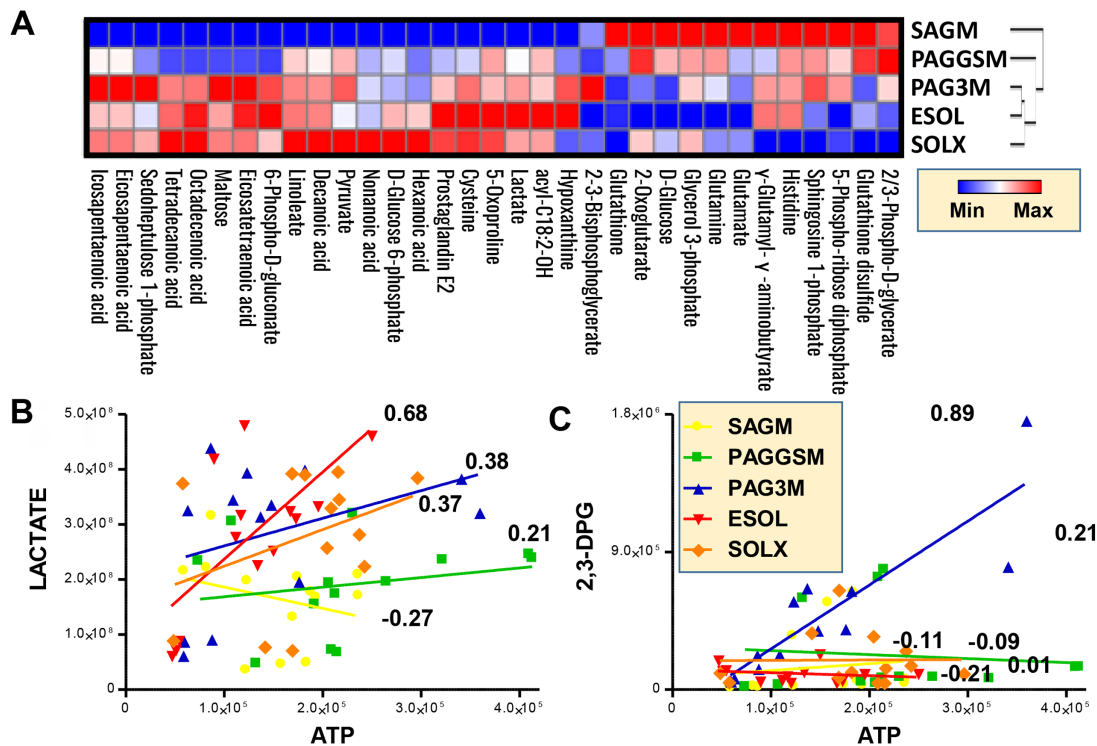


Fig. 5. Top metabolic correlates to ATP across all additive solutions, plotted as a hierarchically clustered heat map (A). (B, C) Linear Spearman correlations (numbers in each panel) of lactate and 2,3-DPG to ATP in each one of the additive, graphed according to the color code in C. [Color figure can be viewed at wileyonlinelibrary.com]

they reconcile *ex vivo* metabolomics observations with potentially clinically relevant outcomes. In this view, an improved additive solution for storage of RBCs should mitigate the metabolic lesion in order to reduce hemolysis and boost posttransfusion recoveries.

In the present study, we generated metabolomics data on five storage additives, including SAGM, the canonical European storage solution, and more recently introduced PAGGSM, as well as three alkaline additives (SOLX, E-SOL 5, and PAG3M). Of note, results on SAGM and PAGGSM we report here are consistent with findings reported by Rolfsson and colleagues,³⁹ who also explored the metabolic impact of other nonalkaline additives such as AS-1 and AS-3, but did not focus on the impact of intracellular alkalinization on stored erythrocyte metabolism. Intracellular alkalinization is achieved in these additives by exploiting the chloride shift concept, by eliminating chloride anions from the formulation balanced by either high bicarbonate loading (SOLX), high citrate and phosphate (E-SOL 5), or membrane-impermeant gluconate (PAG3M). Theoretically, the chloride-efflux effect induced by incorporation of gluconate in the additive should be reversible once anionic equilibrium is reached, unlike the chloride efflux induced by low/no-chloride high-bicarbonate additives. However, the chloride shift impact of gluconate (as determined by measurements of

bicarbonate and chloride anions; Fig. S2) perfectly overlaps in the alkaline additives PAG3M, E-SOL 5, and SOLX. Still, the gluconate-containing additive (PAG3M) showed the highest DPG levels through the whole storage period, suggesting that phenomena other than alkalinization alone (i.e., fueling of late glycolysis by pentose phosphate compounds released via phosphoribolysis of guanosine) may contribute to the beneficial activation of the Rapoport-Luebering shunt. Classic biochemical understanding of RBC energy metabolism posits that the synthesis of 2,3-DPG through the Rapoport-Luebering shunt “sacrifices” the generation of one molecule of ATP.⁵⁷ While this held true also in the present study for all storage additives, including alkaline- and guanosine-containing additives, gluconate-containing PAG3M was the only additive showing significant positive correlations between the levels of ATP and 2,3-DPG, highlighting a metabolic peculiarity of RBCs stored in presence of the PAG3M formula.

Intracellular alkalinization is anticipated to boost glycolysis, the PPP, and the Rapoport-Luebering pathway through the pH-dependent increases in the activity of the rate-limiting enzymes phosphofructokinase, glucose-6-phosphate dehydrogenase, and bisphosphoglycerate mutase.¹⁵ Here, we show that decreased RBC spiculation (i.e., formation of morphologically altered echinocytes) and hemolysis are observed in alkaline additives, a

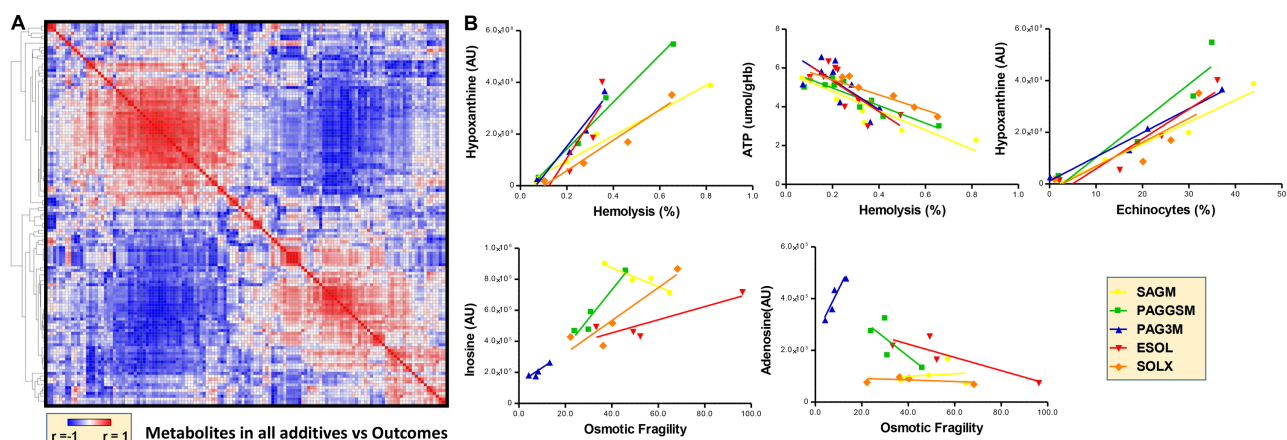


Fig. 6. Correlation matrix of all metabolites to outcomes (A) and highlight of top metabolic correlates to hemolysis, morphology and osmotic fragility across all additives. Purines, especially adenosine and its deamination products inosine and hypoxanthine were the best correlates to all tested functional outcomes independently (top row) or dependently (bottom row) on the additive solution. Color code in the bottom right corner of the figure identifies linear correlation curves across all additives at all tested time points. [Color figure can be viewed at wileyonlinelibrary.com]

phenomenon that correlated with reduced ATP breakdown and purine deamination rather than free fatty acids and fatty acid oxidation. This observation, while preliminary, is suggestive of the fact that preserved energy homeostasis mitigates RBC spiculation, a “save or sacrifice” phenomenon to eliminate oxidation products (including oxidized lipids). However, preserved energy homeostasis in alkaline additives (especially PAG3M and E-SOL 5) is not sufficient to completely prevent lipid oxidation, for which introduction of hydrophilic (e.g., ascorbate) or lipophilic (e.g., vitamin E) antioxidants may represent a better option.³⁰⁻³⁴ An alternative explanation to this phenomenon is an increase in oxidized lipid recycling through the Lands cycle, a phenomenon that is promoted by hypoxia⁵⁸ and may be similarly affected by alkalization.

On the other hand, alkaline additives effectively prevented purine deamination, especially in the case of PAG3M. Of note, introduction of guanosine to the additive formulation of PAGGSM and PAG3M ended up boosting the guanine nucleotide pool and fueling ATP generation with no initial energy investment in late glycolysis via phosphoribolysis, rather than generation of inosine through the activity of hypoxanthine guanosine phosphoribosyl transferase. Lower levels of hypoxanthine and higher ratios of nondeaminated to deaminated purines (e.g., ATP/hypoxanthine) or decreased purine oxidation catabolites (urate/hypoxanthine) were indeed observed in all alkaline additives, especially in PAG3M, SOLX, and E-SOL 5 (in that order).

Increased phosphoribolysis may also explain the observed increases in steady-state levels of nonoxidative-phase PPP metabolites (e.g., sedoheptulose

phosphate). This observation could also be alternatively explained by increased fluxes through the oxidative PPP, resulting in higher nonoxidative/oxidative PPP intermediate ratios (consistent with higher glucose-6-phosphate dehydrogenase activity and thus increased antioxidant capacity in alkaline RBCs). Indeed, we recently appreciated the role that oxidative stress plays in activating AMP deaminase 3 to promote purine deamination and thus hypoxanthine accumulation, a phenomenon that negatively correlates with posttransfusion recovery and is prevented by hypoxic storage (which also induces intracellular alkalization).²⁴ However, direct comparison of hypoxanthine levels in alkaline versus nonalkaline additives (SOLX vs. AS-3) in unpaired studies showed increases in the former group, also accompanied by higher total levels of nondeaminated purines and ATP.⁴⁵ Similarly, supplementation of CO₂ to hypoxically stored RBCs decreased hypoxanthine levels but increased urate/hypoxanthine ratios. This suggests a role of alkalization in preventing hypoxanthine catabolism or a phenomenon independent from alkalization in explaining hypoxia-induced decreases in RBC hypoxanthine.⁵⁷ Similarly, it must be noted that, unlike RBCs, mitochondria-endowed cells generate hypoxanthine under hypoxic conditions, a caveat that would recommend caution when considering purine deamination-related data on hypoxic storage of RBCs in the presence of residual WBCs (while the leukoreduced RBC units used for this study have $<0.1 \times 10^6$ WBCs). Alternatively, ATP/hypoxanthine ratios, or hypoxanthine metabolism to urate and hydrogen peroxide, rather than hypoxanthine levels per se, may be candidate markers of the RBC metabolic lesion for future studies. Finally, activation of

purinergic signaling via adenosine receptors has been shown to boost RBC glycolysis and DPG generation in vivo and ex vivo, a phenomenon that may be leveraged to further promote purine homeostasis in stored RBCs under (alkaline) normoxic or hypoxic conditions.⁵⁹ Future additives may contain antioxidants to promote energy metabolism via inhibition of purine deamination by redox-sensitive deaminases, although antioxidants other than ascorbates or sugars other than glucose should be included in those formulations to avoid the negative effect on glycolysis triggered by competitive uptake of glucose and dehydroascorbate by glucose transporter 1.³⁰

CONCLUSION

In the present study, we provided the first comparative metabolomics analysis of RBCs stored in different alkaline additives SOLX, E-SOL 5, and PAG3M or in nonalkaline/classic additives such as SAGM or PAGGSM. The results from our metabolic analyses indicate superior RBC preservation in PAG3M as compared to the other alkaline additives and, in general, in alkaline additives as compared to nonalkaline SAGM and PAGGSM. In particular, DPG and ATP generation and maintenance, as well as purine metabolism and redox homeostasis (especially the PPP and its nonoxidative-phase by-products) were favorable in PAG3M and other alkaline additives in comparison to SAGM and PAGGSM. However, the observed metabolic benefits do not extend to the prevention of storage-induced fatty acid release and lipid oxidation. The correlation of metabolites from these pathways with surrogate ex vivo indexes of functional outcomes (e.g., cell morphology and osmotic fragility) are relevant in that they confirm and extend the recent observation on the (correlative) role of purine deamination in RBC recovery after transfusion.²⁴ However, additional functional in vivo measurements (e.g., posttransfusion recovery) will be instrumental to further expand our understanding of the impact of these storage additives on transfusion efficacy. Results from the present study provide additional insights in the metabolic benefits of alkaline storage additives and will likely guide the formulation of novel additives in the near future.

ACKNOWLEDGMENTS

Research reported in this publication was supported in part by funds from the Boettcher Webb-Waring Biomedical Research Award—Early Career grant (ADA) and the Shared Instrument grant by the National Institutes of Health (S10OD021641).

ADA, RVB, and DDK designed the study. HK, RVB, and DDK generated the samples. RCH, JAR, and ADA performed metabolomics analyses. ADA wrote the first draft of the manuscript, and all the authors contributed to its finalization.

CONFLICT OF INTEREST

ADA is a founder of Omix Technologies, Inc., and a consultant for New Health Sciences, Inc. All the remaining authors have disclosed no conflicts of interest.

REFERENCES

1. Mollison PL. The introduction of citrate as an anticoagulant for transfusion and of glucose as a red cell preservative. *Br J Haematol* 2000;108:13-8.
2. Greenwalt TJ. A short history of transfusion medicine. *Transfusion* 1997;37:550-63.
3. Hess JR. An update on solutions for red cell storage. *Vox Sang* 2006;91:13-9.
4. Ellingson KD, Sapiano MRP, Haass KA, et al. Continued decline in blood collection and transfusion in the United States—2015. *Transfusion* 2017;57(Suppl 2):1588-98.
5. Högman CF, Hedlund K, Sahleström Y. Red cell preservation in protein-poor media. III. Protection against in vitro hemolysis. *Vox Sang* 1981;41:274-81.
6. Heaton A, Miripol J, Aster R, et al. Use of Adsol preservation solution for prolonged storage of low viscosity AS-1 red blood cells. *Br J Haematol* 1984;57:467-78.
7. Simon TL, Marcus CS, Myhre BA, et al. Effects of AS-3 nutrient-additive solution on 42 and 49 days of storage of red cells. *Transfusion* 1987;27:178-82.
8. Cicha I, Suzuki Y, Tateishi N, et al. Gamma-ray-irradiated red blood cells stored in mannitol-adenine-phosphate medium: rheological evaluation and susceptibility to oxidative stress. *Vox Sang* 2000;79:75-82.
9. Walker WH, Netz M, Gänshirt KH. 49 day storage of erythrocyte concentrates in blood bags with the PAGGS-mannitol solution. *Beitr Zur Infusionstherapie Contrib Infus Ther* 1990;26:55-9.
10. Cancelas JA, Dumont LJ, Maes LA, et al. Additive solution-7 reduces the red blood cell cold storage lesion. *Transfusion* 2015;55:491-8.
11. Radwanski K, Thill M, Min K. Red cell storage in E-Sol 5 and Adsol additive solutions: paired comparison using mixed and non-mixed study designs. *Vox Sang* 2014;106:322-9.
12. Hess JR, Hill HR, Oliver CK, et al. Alkaline CPD and the preservation of RBC 2,3-DPG. *Transfusion* 2002;42:747-52.
13. Hess JR, Rugg N, Joines AD, et al. Buffering and dilution in red blood cell storage. *Transfusion* 2006;46:50-4.
14. Meryman HT, Hornblower M, Keegan T, et al. Refrigerated storage of washed red cells. *Vox Sang* 1991;60:88-98.
15. Nemkov T, Hansen KC, Dumont LJ, et al. Metabolomics in transfusion medicine. *Transfusion* 2016;56:980-93.
16. Cotterrell D, Whittam R. The influence of the chloride gradient across red cell membranes on sodium and potassium movements. *J Physiol* 1971;214:509-36.
17. Burger P, Korsten H, De Korte D, et al. An improved red blood cell additive solution maintains 2,3-diphosphoglycerate and adenosine triphosphate levels by an enhancing

- effect on phosphofructokinase activity during cold storage. *Transfusion* 2010;50:2386-92.
18. de Korte D, Kleine M, Korsten HGH, et al. Prolonged maintenance of 2,3-diphosphoglycerate acid and adenosine triphosphate in red blood cells during storage. *Transfusion* 2008;48:1081-9.
 19. Mays JA, Hess JR. Modelling the effects of blood component storage lesions on the quality of haemostatic resuscitation in massive transfusion for trauma. *Blood Transfus* 2017;15:153-7.
 20. Dumont LJ, AuBuchon JP. Evaluation of proposed FDA criteria for the evaluation of radiolabeled red cell recovery trials. *Transfusion* 2008;48:1053-60.
 21. de Korte D. New additive solutions for red cells. *ISBT Sci Ser* 2016;11:165-70.
 22. Paglia G, D'Alessandro A, Rolfsson Ó, et al. Biomarkers defining the metabolic age of red blood cells during cold storage. *Blood* 2016;128:e43-50.
 23. Paglia G, Sigurjónsson ÓE, Bordbar A, et al. Metabolic fate of adenine in red blood cells during storage in SAGM solution. *Transfusion* 2016;56:2538-47.
 24. Nemkov T, Sun K, Reisz JA, et al. Hypoxia modulates the purine salvage pathway and decreases red blood cell and supernatant levels of hypoxanthine during refrigerated storage. *Haematologica* 2018;103:361-72.
 25. Casali E, Berni P, Spisni A, et al. Hypoxanthine: a new paradigm to interpret the origin of transfusion toxicity. *Blood Transfus* 2015;14:555-6.
 26. D'Alessandro A, Gray AD, Szczepiorkowski ZM, et al. Red blood cell metabolic responses to refrigerated storage, rejuvenation, and frozen storage. *Transfusion* 2017;57:1019-30.
 27. Fagiolo E, Littarru GP, Lippa S, et al. Biochemistry of packed red blood cell concentrates stored in PAGGS-sorbitol solution for 42 days. *Vox Sang* 1987;52:301-4.
 28. Rolfsson Ó, Johannsson F, Magnúsdóttir M, et al. Mannose and fructose metabolism in red blood cells during cold storage in SAGM. *Transfusion* 2017;57:2665-76.
 29. Park TJ, Reznick J, Peterson BL, et al. Fructose-driven glycolysis supports anoxia resistance in the naked mole-rat. *Science* 2017;356:307-11.
 30. Pallotta V, Gevi F, D'Alessandro A, et al. Storing red blood cells with vitamin C and N-acetylcysteine prevents oxidative stress-related lesions: a metabolomics overview. *Blood Transfus* 2014;12:376-87.
 31. Vani R, Soumya R, Carl H, et al. Prospects of vitamin C as an additive in plasma of stored blood. *Adv Hematol* 2015;2015:961049.
 32. Czubak K, Antosik A, Cichon N, et al. Vitamin C and Trolox decrease oxidative stress and hemolysis in cold-stored human red blood cells. *Redox Rep* 2017;22:445-50.
 33. Sanford K, Fisher BJ, Fowler E, et al. Attenuation of red blood cell storage lesions with vitamin C. *Antioxidants (Basel)* 2017;6.
 34. Silva CAL, Azevedo Filho CA, Pereira G, et al. Vitamin E nanoemulsion activity on stored red blood cells. *Transfus Med Oxf Engl* 2017;27:213-7.
 35. Fu X, Felcyn JR, Zimring JC. Bioactive lipids are generated to micromolar levels during RBC storage, even in leukoreduced units. *Blood* 2015;126:2344.
 36. D'Alessandro A, Dzieciatkowska M, Nemkov T, et al. Red blood cell proteomics update: is there more to discover? *Blood Transfus* 2017;15:182-7.
 37. Bryk AH, Wiśniewski JR. Quantitative analysis of human red blood cell proteome. *J Proteome Res* 2017;16:2752-61.
 38. D'Alessandro A, Nemkov T, Yoshida T, et al. Citrate metabolism in red blood cells stored in additive solution-3. *Transfusion* 2017;57:325-36.
 39. Rolfsson Ó, Sigurjónsson ÓE, Magnúsdóttir M, et al. Metabolomics comparison of red cells stored in four additive solutions reveals differences in citrate anticoagulant permeability and metabolism. *Vox Sang* 2017;112:326-35.
 40. Nemkov T, Sun K, Reisz JA, et al. Metabolism of citrate and other carboxylic acids in erythrocytes as a function of oxygen saturation and refrigerated storage. *Front Med* 2017;4:175.
 41. D'Alessandro A, Kriebardis AG, Rinalducci S, et al. An update on red blood cell storage lesions, as gleaned through biochemistry and omics technologies. *Transfusion* 2015;55:205-19.
 42. Roback JD, Josephson CD, Waller EK, et al. Metabolomics of AS-1 RBC storage. *Transfus Med Rev* 2014;28:41-55.
 43. D'Alessandro A, Nemkov T, Kelher M, et al. Routine storage of red blood cell (RBC) units in additive solution-3: a comprehensive investigation of the RBC metabolome. *Transfusion* 2015;55:1155-68.
 44. D'Alessandro A, Hansen KC, Silliman CC, et al. Metabolomics of AS-5 RBC supernatants following routine storage. *Vox Sang* 2015;108:131-40.
 45. D'Alessandro A, Nemkov T, Hansen KC, et al. Red blood cell storage in additive solution-7 preserves energy and redox metabolism: a metabolomics approach. *Transfusion* 2015;55:2955-66.
 46. Lagerberg JW, Korsten H, Van Der Meer PF, et al. Prevention of red cell storage lesion: a comparison of five different additive solutions. *Blood Transfus* 2017;15:456-62.
 47. Nemkov T, Hansen KC, D'Alessandro A. A three-minute method for high-throughput quantitative metabolomics and quantitative tracing experiments of central carbon and nitrogen pathways. *Rapid Commun Mass Spectrom RCM* 2017;31:663-73.
 48. Xia J, Sinelnikov IV, Han B, et al. MetaboAnalyst 3.0—making metabolomics more meaningful. *Nucleic Acids Res* 2015;43:W251-7.
 49. D'Alessandro A, Nemkov T, Reisz J, et al. Omics markers of the red cell storage lesion and metabolic linkage. *Blood Transfus* 2017;15:137-44.
 50. Blasi B, D'Alessandro A, Ramundo N, et al. Red blood cell storage and cell morphology. *Transfus Med Oxf Engl* 2012;22:90-6.
 51. Reisz JA, Wither MJ, Dzieciatkowska M, et al. Oxidative modifications of glyceraldehyde 3-phosphate dehydrogenase

- regulate metabolic reprogramming of stored red blood cells. *Blood* 2016;128:e32-42.
52. Zimring JC. Widening our gaze of red blood storage haze: a role for metabolomics. *Transfusion* 2015;55:1139-42.
 53. de Wolski K, Fu X, Dumont LJ, et al. Metabolic pathways that correlate with post-transfusion circulation of stored murine red blood cells. *Haematologica* 2016;101:578-86.
 54. Van't Erve TJ, Wagner BA, Martin SM, et al. The heritability of hemolysis in stored human red blood cells. *Transfusion* 2015;55:1178-85.
 55. Dumont LJ, D'Alessandro A, Szczepiorkowski ZM, et al. CO₂-dependent metabolic modulation in red blood cells stored under anaerobic conditions. *Transfusion* 2016;56:392-403.
 56. Wu H, Bogdanov M, Zhang Y, et al. Hypoxia-mediated impaired erythrocyte Lands' cycle is pathogenic for sickle cell disease. *Sci Rep* 2016;6:29637.
 57. Sun K, D'Alessandro A, Xia Y. Purinergic control of red blood cell metabolism: novel strategies to improve red cell storage quality. *Blood Transfus* 2017;15:535-542. 

SUPPORTING INFORMATION

Additional Supporting Information may be found in the online version of this article at the publisher's website.

Fig. S1. Functional outcomes, including hemolysis (percentage), osmotic fragility curves, morphology (percentage of echinocytes), and apoptotic cells (phosphatidylserine exposure prior to and after incubation at 37°C). Graphs indicated line plots (median \pm range) for each different

additive, following the color scheme in the bottom right corner of the figure.

Fig. S2. Gas measurements, hematological parameters and ion homeostasis during storage in all different additives (tested on a weekly basis from Storage Day 1 to 56 – *x* axis). Graphs indicated line plots (median \pm range) for each different additive, following the color scheme on the right-hand side of the figure.

Fig. S3. Vectorial version of hierarchical clustering analyses of time course measurements of RBC metabolites at Storage Days 1, 21, 35, and 56 in five different storage additives.

Fig. S4. 2-dimensional plots of principal component analysis (PC), showing PC1 versus PC2, PC1 versus PC3, and PC2 versus PC3.

Fig. S5. Glutathione homeostasis. Graphs indicated line plots (median \pm range) for each different additive, following the color scheme of all the figures presented in this manuscript.

Fig. S6. Fatty acid and eicosanoids (significant changes across additives and during storage). Graphs indicated line plots (median \pm range) for each different additive, following the color scheme of all the figures presented in this manuscript.

Fig. S7. Vectorial version of the correlation matrix of metabolite and outcomes, independently from the additive solution tested.

Table S1. Metabolomics measurements in RBCs stored in different standard and alkaline additives.

Table S2. Correlation Matrix between metabolic phenotypes and functional measurements in RBCs stored in standard and alkaline additives.